KS10076, metal chelator, enhances radiation sensitivity via ROS-mediated ER stress pathway in triple-negative breast cancer

Danbi Yu

Department of Medicine

The Graduate School, Yonsei University

KS10076, metal chelator, enhances radiation sensitivity via ROS-mediated ER stress pathway in triple-negative breast cancer

Directed by Professor Sang Joon Shin

The Master's Thesis
submitted to the Department of Medicine,
the Graduate School of Yonsei University
in partial fulfillment of the requirements for the degree
of Master of Medical Science

Danbi Yu

June 2022

This certifies that the Master's Thesis of
Danbi Yu is approved.

[Signature]

Thesis Supervisor: Sang Joon Shin

[Signature]

Thesis Committee Member#1: Minkyu Jung

[Signature]

Thesis Committee Member#2: Hong In Yoon

The Graduate School
Yonsei University

June 2022

ACKNOWLEDGEMENTS

지난 2년동안 기쁘고 힘들었던 많은 일들이 있었지만 지나고 보니 모두 행복했던 추억입니다.

먼저, 석사학위 과정 동안 제가 연구를 끝맺음 할 수 있도록 도와주신 신상준 교수님께 매우 감사 드립니다. 교수님의 끊임없는 지도와 격려 덕분에 흔들리지 않고 묵묵히 저의 길을 걸어갈 수 있게 되었던 것 같습니다. 처음 입학하였을 때 교수님의 모습이 선명하게 기억납니다.
연구하는 것을 진심으로 행복해 하시고, 열정 가득한 눈빛으로 저희를 바라보며 좋은 말씀을 많이 건내 주셨기 때문에, 존경하는 마음을 안고 교수님과 2년동안 함께할 수 있었습니다. 정말 감사드립니다.

또한 바쁘신 와중에도 논문 심사로 시간 내어주신 정민규 교수님, 윤홍인 교수님께도 감사드립니다. 교수님들의 심사 의견 덕분에 한층 더 발전하는 방향으로 연구할 수 있었습니다. 정말 감사드립니다.
그리고, 지난 2년간 함께 동고동락했던 우리 실험실 동기 효정이, 선배 지언 박사님, 우영 선생님, 후배 진우, 형주, 정윤, 예영이 그리고 향화 언니, 수민 선생님, 이솜 선생님께도 감사합니다. 모두들 덕분에 즐겁고

행복하게 연구실 생활할 수 있었습니다.

그리고, 늘 따뜻한 사랑으로 언제나 제 편이 되어준 우리 아빠, 엄마, 지형이, 할머니, 외할머니, 이모와 항상 저를 위해 기도해주시는 가족들 모두 다 감사드립니다. 아낌없이 주신 사랑 베풀면서 살아가도록 하겠습니다. 곁에서 늘 위로해주고 힘이 되어준 희진이에게도 고맙단 말 전합니다. 존재만으로도 나한텐 너무 큰 행운이야.

마지막으로 지난 겨울 별이 된 우리 할아버지, 할아버지께서 말씀해주신 것들 늘 새기며 살아가겠습니다. 사랑합니다.

TABLE OF CONTENTS

LIST OF FIGURES

ABSTRACT

KS10076, metal chelator, enhances radiation sensitivity via ROS-mediated ER stress pathway in triple-negative breast cancer

Danbi Yu

Department of Medicine
The Graduate School, Yonsei University

(Directed by Professor Sang Joon Shin)

Among breast cancer, the most aggressive and deadly triple-negative breast cancer (TNBC) is known to be resistant to radiation therapy (RT), and many studies have reported that the STAT3 protein is involved in its resistance. However, the mechanisms underlying the development of resistance to therapy are not fully understood. In this study, for the first time, radioresistance was investigated in breast cancer cells as an examining the crosstalk between the activation of STAT3 and ER stress. As a result, we discovered that TNBC cells with high expression of pSTAT3 did not induce ER stress due to the lack of ROS generated by radiation alone. On the other hand, non-TNBC cells with low expression of pSTAT3 induced ER stress via increasing ROS levels. Furthermore, combined treatment of KS10076, a metal chelator, and radiation remarkably caused ER stress via the inhibition of pSTAT3 expression and the generation of ROS in TNBC cells, which eventually resulted in hyperactivation of apoptosis and autophagy. These results demonstrated that KS10076 reverses radiation resistance the elevation of ROS-mediated ER stress. Taken together,

our findings reveal mechanisms mediating radiation resistance and provide a KS10076 combinatorial strategy to overcome radiation resistance in TNBC cells.

Key words: TNBC, STAT3, radiation, ROS, metal chelator, ER stress

KS10076, metal chelator, enhances radiation sensitivity via ROS-mediated ER stress pathway in triple-negative breast cancer.

Danbi Yu

Department of Medicine
The Graduate School, Yonsei University

(Directed by Professor Sang Joon Shin)

I. INTRODUCTION

Triple-negative breast cancer (TNBC) is the most aggressive subtype among breast cancer (BC) and accounts for 70% of BC-related mortality[1]. However, TNBC is insensitive to hormone nor HER2-targeted therapy due to a lack of estrogen or progesterone receptors as well as HER2 protein[2]. Nevertheless, there is no targeted therapy used in the clinic for TNBC treatment[3,4]. Radiotherapy (RT) can be used to treat all stages of breast cancer (BC) and an effective way after mastectomy, but TNBC patients are more likely to acquire radioresistance[5,6]. Accordingly, radiation treatment can have detrimental effects on a TNBC patients through a higher recurrence rate, and a poor response to subsequent treatments after RT compared to other BC patients. So far, mechanisms involved in TNBC radioresistance remain poorly understood and there is unknown clinically effective radiation-sensitizer for the treatment of TNBC patients. On this front, elucidating the mechanism of TNBC radioresistance and discovering potential drugs that can improve the radiosensitivity of TNBC has significant clinical value.

Signal transducer and activator 3 (STAT3) is a transcription factor that activates downstream genes involved in various processes, such as cell proliferation, survival, and metastasis in cancer cells. Importantly, STAT3

frequently activated oncogene in TNBC and plays a critical role in TNBC progression[7-9]. Previous studies have attributed the cause of radioresistance to the continuous activation of the STAT3 pathway in TNBC cells leading to the blockage of ROS and the activation of Survivin, an anti-apoptotic protein[10-12]. In this way, activation of STAT3 plays a key role in radioresistance, and thus, pSTAT3 was deemed an attractive therapeutic target for enhancing radiosensitivity.

Accumulating evidence indicates that radiation interacts with water molecules to form oxonium ions and a free radical[13,14]. These highly active molecules then react form hydroxyl radical or other ROS species. On the other hands, our previous study reported that KS10076, a metal chelator, interacted with iron or on cancer cells[32]. KS10076 disrupted redox-active iron complexes resulting in the generation of ROS and the subsequent degradation of STAT3. As the mechanism of ROS generation by radiation and KS10076 is distinct, we hypothesized that combination therapy could significantly enhance ROS levels to overcome radioresistance.

In this study, we first examined radiation sensitivity between TNBC and non-TNBC cells, then observed that TNBC cells have lower radiosensitivity than non-TNBC cells. A recent study demonstrated that STAT3 is highly activated in TNBC cells suggesting that STAT3 promote radioresistance in TNBC cells[10-12]. However, the role of STAT3 and its mechanism of resistance associated with cell death in TNBC remain fully unknown. Thus, we elucidated the mechanisms underlying how STAT3 regulated radioresistance through the ROS-mediated ER stress in TNBC cells. Hence, we demonstrated a novel therapeutic strategy to induce ER stress in TNBC cells.

II. Materials and methods

1. Cell culture studies.

Human breast MDA-MDA-231, HCC-1937, MDA-MB-453, SK-BR-3 and MCF-7 cells were purchased from Korean Cell Line Bank (Seoul, South Korea) and MDA-MB-468 cells was purchased from ATCC (Manassas, USA). MDA-MDA-231, HCC-1937, MDA-MB-453, SK-BR-3 and MCF-7 cells were maintained in RPMI Medium (Lonza, Basel, Switzerland) while MDA-MB-468 was maintained in DMEM (Lonza, Basel, Switzerland) supplemented with 10% fetal bovine serum, 100 IU/mL penicillin and 100 μg/mL in a 37℃ incubator containing 5% CO_2.

2. Cell viability assay

A CCK-8 kit (Dojindo, Kumamoto, Japan) was used to evaluate the cell viability, according to the manufacturer`s instructions. The cells were incubated into 96-well plates. After the cells adhered to the walls of the culture plate, Dp44mT (Sigma, Missouri, USA) or KS10076 or radiation were added to each well for 48 h, then the CCK-8 reagent was added into 96-well plates (10 μL/well) and incubated at 37℃ for 3-4 h. The absorbance was measured at 450 nm wavelength. IC_{50} values were calculated using GraphPad Software (San Diego, CA, USA). KS10076 was provided from Korea Research Institute of Chemical Technology (KRICT) (Daejeon, South Korea) and was diluted in DMSO.

3. Western blot

Total cell lysate was lysed radioimmunoprecipitation assay (RPPA, ELPIS-BIOTECH, Daejeon, South Korea) buffer containing phosphatase and protease inhibitors. Protein concentration was detected by bovine serum albumin (BSA) standard concentration. Equal amounts of protein lysate were

loaded onto 96 well plate and then transferred onto polyvinylidene fluoride (PVDF) membrane. After blocking with 1% BSA in Tris buffered saline (TBS) containing 0.1% Tween-20, the membranes were incubated overnight at 4 °C with the following primary antibodies from Cell Signaling (Massachusetts, Danvers, USA): pSTAT3(Y705) (#9145), STAT3 (#9139), Survivin (#2808), XIAP (#2042), PERK (#3192), peIF2a (#9721), ATF4(#11815), CHOP (#2895) and antibodies from santa cruz biotechnology (Dallas, Texas, USA): β-actin (sc-47778), GAPDH (sc-32233). After washing with TBS containing 0.1% Tween-20, blots were incubated with horseradish peroxidase (HRP)-conjugated anti-mouse and anti–rabbit secondary antibodies (Thermo Scientific, Waltham, Massachusetts, USA). Blots were developed using the enhanced chemiluminescence (ECL) system (ECL Plus; Thermo Scientific, USA). The intensity of the bands was quantified with graphpad software. MitoQ was purchased from MedchemExpress (MCE, New Jersey, USA) and was diluted in DMSO. To assess mitochondrial ROS scavenge, cells were pre-treated for 1 h with 1 μM MitoQ (MCE, USA).

4. Flow cytometry assay

Cells were detected by flow cytometry with DCFDA or Mito-SOX solution using BD FACS LSR II SORP system (Becton Dickinson, Franklin Lakes, NJ, USA). For evaluation of apoptosis, cells were labeled with the PE Annexin V Apoptosis Detection Kit (Thermo Scientific, USA) following the manufacturer's protocol. Briefly, cells were pelleted and resuspended in binding buffer and incubated for 15 min at room temperature. For DCFDA fluorescence, cells were labeled with the DCFDA Cellular ROS detection assay kit (Thermo Scientific, USA) as instructed by the manufacturer's protocol. Briefly, cells were stained with 3 μM DCFDA for 30 min at 37 °C in the dark. For Mito-SOX fluorescence, cells were labeled with Mito-SOX Red mitochondrial superoxide indicator (Thermo Scientific, USA) in 5 μM concentration for 30 min at 37 °C

in the dark. After incubation, cells were washed with PBS two times and analyzed on FACS.

5. Colony formation assay

For colony formation, cells were seeded and cultured with appropriate medium for 2 weeks. After being fixed with 100% methanol for 10 min and stained with crystal violet for 70 min, the number of colonies was calculated with Image J software (NIH, USA).

6. Transfection assay

MCF-7 cells were transfected STAT3 plasmid (Korea Human Gene Bank, Daejeon, South Korea) using Lipofectamine 2000 (Thermo Scientific, USA) following the manufacturer's instructions. To knock down ATF4, cells were cultured at 60-70% confluence and transfected for 48 h with siATF4 using RNAiMAX (Thermo Scientific, USA) according to manufacturer's protocols. Cells were treated with KS10076 or radiation at 48 h after transfection. siRNA synthesized in IDT (Integrated DNA Technologies, New Jersey, USA)

7. Immunoflourescence assays

Cells were fixed with 4% paraformaldehyde in PBS (pH = 7.4) for 15 min at room temperature. After washing three times with PBS-T, the cells were permeabilized with 0.1% Triton-X100 (Sigma, USA) for 15 min. After the wash with PBS-T, the cells were incubated with blocking solution (3% BSA) for 30 min and primary antibody for LC3B (Novus Biologicals, NB100-2220) overnight 4℃. After three 5 min washing in PBS-T, cells were incubated with secondary antibodies (1:1000) and DAPI (500nM) for 1 h at 25 ℃ and washed again twice with PBS-T washes for 10 min. The samples with 3 biological replicates were imaged using Operetta CLS instrument (PerkinElmer, Waltham, Massachusetts, USA) at 6 fields randomly selected.

8. Animal models and radiation exposure

Nude mice (female, 6 weeks old) were obtained from Orient Bio Inc (Seongnam-si, South Korea) and were housed in pressurized, ventilated cages with standard rodent chow, water, and a 12 h light/dark cycle. After the adaptation period, xenografts were implanted by subcutaneous injection into the fat pad of mice with 0.2 mL of MDA-MB-231 cell suspensions (1.5×10^7 cells/mL) in Matrigel / PBS (1:1) mixture. Mice with tumor volume of 300 mm^3 with no abnormality in general health were selected and distributed in to vehicle controls and experimental groups randomly. Mice were treated with radiation 6 Gy (X-Rad, Precision, North Branford, CT, USA) or KS10076 (12.5 mpk) (2 days/week) or combination. All animal experiments were conducted according to the guidelines of the Institutional Animal Care and Use Committee. Results were determined beginning 15 days after irradiation. Tumor volume and body weight were measured every 3 days according to the following formula: Tumor volume = Length (mm) $\times$ Width^2 (mm^2) $\times$ 1/2. At the end of the experiment, tumors were removed, photographed, and processed for western blot analyses. Cells were further treated with 4 Gy radiation (Gammacell Low dose-rate research irradiator, MDS Nordion, Canada).

9. Quantification and statistical analysis

Statistical analyses were conducted using specific statistical tests as indicated in the figure legends using GraphPad 5.01 software for each experiment. All experiments were repeated at least three times, and data are presented as the mean ± standard error of the mean as indicated in the figure legends. Statistical analysis was performed using two-tailed Student`s t-test, One-way ANOVA (Tukey`s) were used to compare differences between groups. Significance is depicted with asterisks on graph as follows: $*p < 0.05$, $**p < 0.01$ and $***p < 0.001$.

III. Results

1. pSTAT3 upregulation mediates radioresistance in breast cancer

To examine the expression of proteins inducing radioresistance, we first analyzed Reverse Phase Protein Array (RPPA) data in breast cancer (BC) cells. The expression of STAT3 protein levels were relatively enriched in TNBC cells (MDA-MB-468 and MDA-MB-231) compared to non-TNBC cells (MDA-MB-453 and MCF-7), and the expression of phosphorylated-STAT3 was higher (Fig. 1A, B). As pSTAT3 is an activated form that directly causes radioresistance, we focused on the role of pSTAT3 expression in the radiosensitivity between TNBC and non-TNBC cells. Therefore, we initially selected TNBC (MDA-MB-468, MDA-MB-231) and non-TNBC (SK-BR-3, MCF-7) cells which do not have mutations in BRCA1 and are androgen receptor negative that can affect radiation resistance[15,16]. To investigate the correlation between STAT3 and radiosensitivity, we evaluated the cell viability and ROS level by radiation (4Gy) in these cell lines. Non-TNBC cells exhibited remarkable cytotoxicity and activation of ROS level compared to TNBC cells (Fig.1C, D). In addition, the population of apoptotic cells increased and ability of colony formation was significantly suppressed in non-TNBC cells, indicating TNBC cells showed radioresistance (Fig.1E, F). Interestingly, the higher expression level of STAT3 and pSTAT3, the lower radiation sensitivity was observed in BC cells (Fig.1B). These finding suggested that expression of STAT3 regulates sensitivity of radiation in BC cells.

2. Elevated pSTAT3 and Survivin contribute to the radioresistant phenotype in TNBC cells.

The persistent activity of STAT3 not only inhibits ROS production but also leads to the upregulation of Survivin, an anti-apoptotic protein, resulting in radioresistance[10-12]. Therefore, we analyzed whether the differences in these protein expressions affected the discrepancy in radiosensitivity between TNBC and non-TNBC cells. The protein expression of STAT3 and Survivin continued to increase in a time-dependent manner in MBA-MB-468 and MDA-MB-231 cells (TNBC cells) (Fig.1G). On the other hand, SK-BR-3 and MCF-7 cell lines (non-TNBC cells) did not have any significant changes (Fig.1G). Taken together, TNBC cells with high expression were exhibited to be more radioresistance than non-TNBC cells through the radiation-induced activation of STAT3 and Survivin. Therefore, we suggested that the expression of pSTAT3 affect radiosensitivity.

A

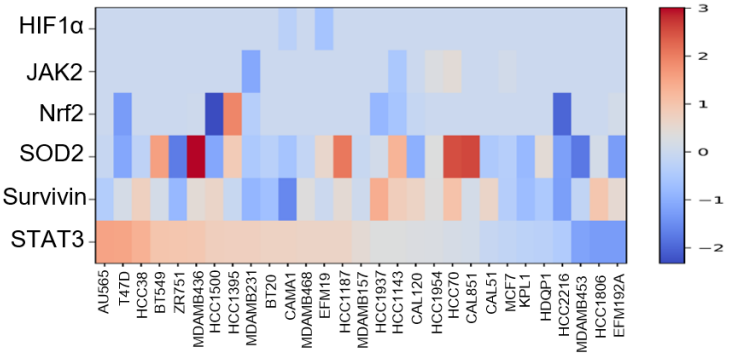

B

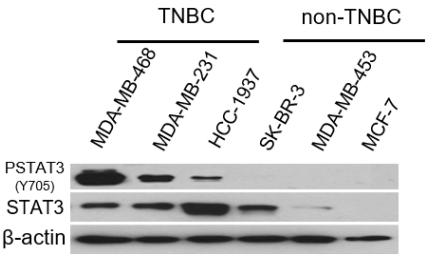

C

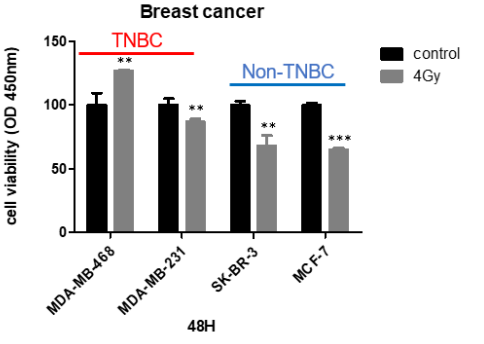

D

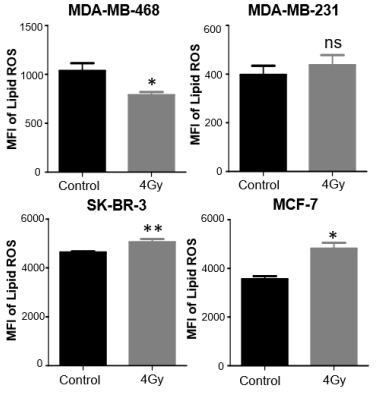

E

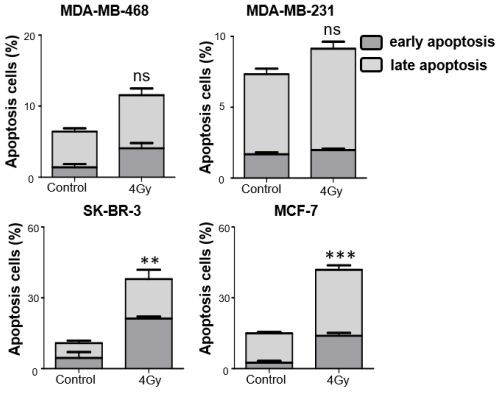

F

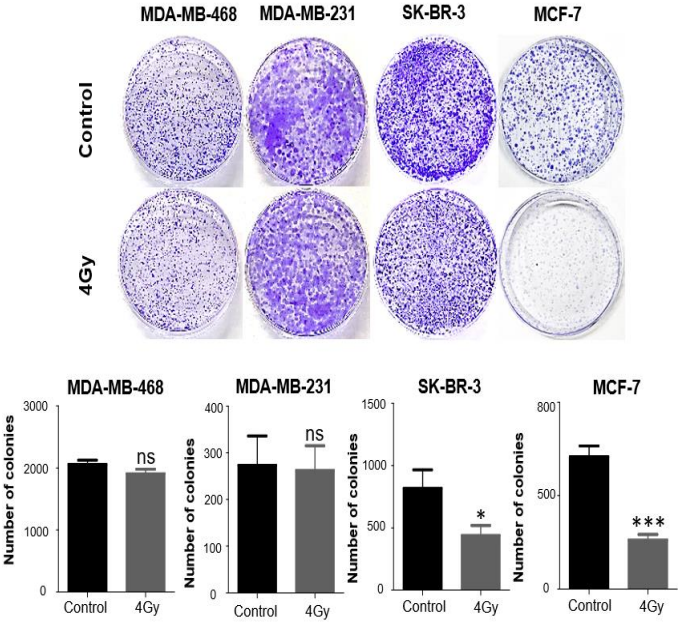

G

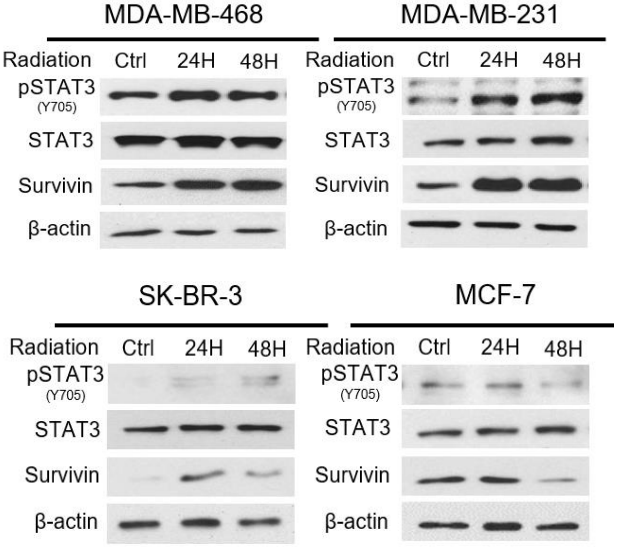

Fig.1 Expression of STAT3 is associated with radioresistance in breast cancer cells. (A) Heatmap of differential protein expression between TNBC and non-TNBC cells using RPPA data. (B) The expression of STAT3 and pSTAT3 in three TNBC and non-TNBC respectively. (C) The percentage of cell viability with the treatment of radiation for 48 h and cell viability was estimated by CCK-8. (D) Cells were treated with 4 Gy radiation. After 48 h, the level of intracellular ROS was determined by measuring the mean fluorescence intensity (MFI) of DCFH-DA (DCF). (E) Cells using Annexin V/PI double staining and analyze using flow cytometry. (F) Clonogenic growth of TNBC (MDA-MB-468, MDA-MB-231) and non-TNBC (SK-BR-3, MCF-7) cells treated with 4 Gy. (G) Protein levels of pSTAT3, STAT3, Survivin in TNBC (MDA-MB-468, MDA-MB-231) and non-TNBC (SK-BR-3, MCF-7) cells treated with 4 Gy radiation. Results are presented as the mean ± standard error from three independent experiments. P value was determined by t-test; ns not significant. ***P<0.001 vs. control **P<0.01 vs. control *P<0.05 vs. control

3. KS10076 inhibits pSTAT3 via ROS generation in TNBC cells.

Our previous study reported that the KS10076, a metal chelator, an analogue of Dp44mT, inhibited STAT3 via promoting ROS[32]. As the binding of a metal chelator to iron induces ROS, we examined the intracellular iron levels using calcein acetoxymethyl ester (AM) in MDA-MB-468 cells. Both of Dp44mT and KS10076 increased the calcein AM that quenched following chelation of metal iron (Fig.2A). Due to the reduction of free iron levels, we examined whether Dp44mT and KS10076 induced ROS levels. The fluorescence intensity of MitoSOX significantly increased after treatment with Dp44mT and KS10076, indicating the elevation of mitochondrial ROS level (Fig.2B).

pSTAT3 inhibits the generation of ROS whereas ROS also inhibits pSTAT3[17,18]. To identify the latter of these dual effects, we treated KS10076 or Dp44mt in MDA-MB-468 cells respectively. While both compounds inhibited pSTAT3, KS10076 showed a more remarkable suppression of pSTAT3 (Fig.2C). As KS10076 had a higher ROS production than Dp44mT (Fig.2B), we hypothesized that KS10076 could more effectively decrease pSTAT3. To clarify whether ROS suppress pSTAT3, we co-treated the mitochondrial ROS scavenger, MitoQ, with both compounds. Despite the two compounds inhibiting pSTAT3, co-treatment with MitoQ rescued pSTAT3 expression (Fig.2D). These findings indicated that the suppression of pSTAT3 by KS10076/Dp44mT was dependent on the generation of ROS.

4. KS10076 improve radiosensitivity of TNBC cells.

We wondered if the KS10076-induced inhibition of pSTAT3 sensitized TNBC cells to radiation. To determine the potential anti-tumor efficacy of KS10076 in BC cells, viability of TNBC cells (MDA-MB-468 and MDA-MB-231) and non-TNBC cells (SK-BR-3 and MCF-7) were evaluated following treatment of KS10076. Interestingly, KS10076 more sensitively suppressed cell viability of TNBC cells than non-TNBC cells (Fig. 2E). These results demonstrated that KS10076 hyperactivates to cells that express high pSTAT3. Additionally, KS10076 had potent cytotoxicity compared with Dp44mT in TNBC cells (Fig.2E, F).

To further explore whether KS10076 affects the sensitivity of radiation to TNBC cells, MDA-MB-468 and MDA-MB-231 cells were co-treated KS10076 and radiation. As a result, pSTAT3 and Survivin proteins, which were persistently up-regulated when treated with radiation alone, were significantly degraded by KS10076 (Fig.1G, 2G). In addition, when the KS10076 and radiation were co-treated, the ROS occurrence revealed a notable trigger than co-treated with Dp44mT at the same concentration (Fig.2H). Thus, these data demonstrated that KS10076 is a synergistically effective drug that is able to increase radiosensitivity.

A

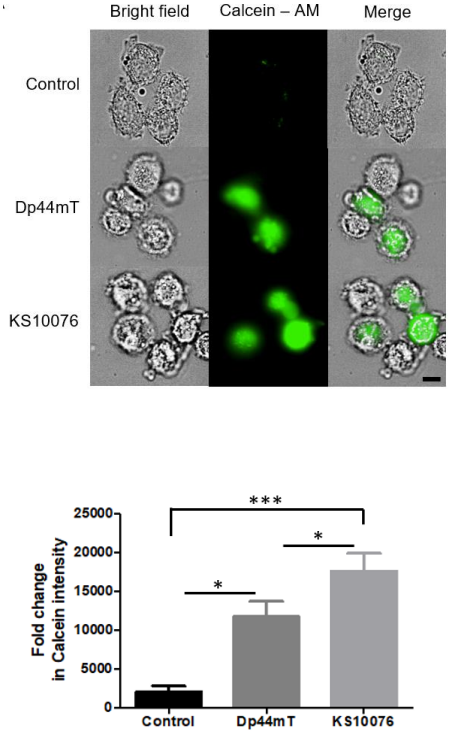

B

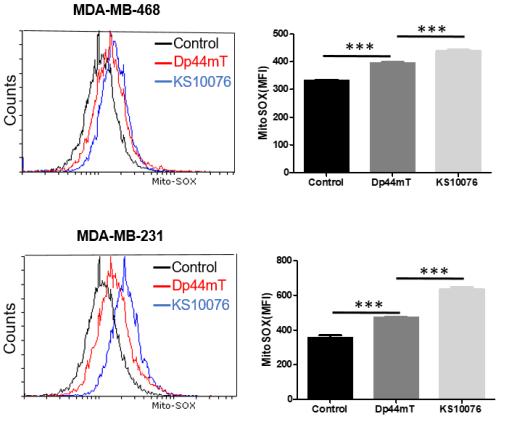

C

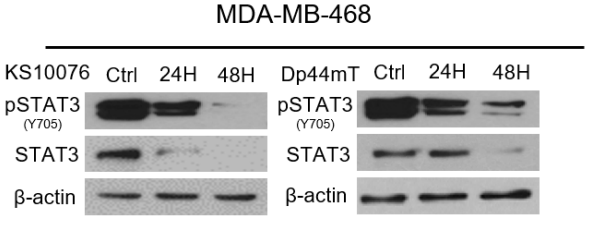

D

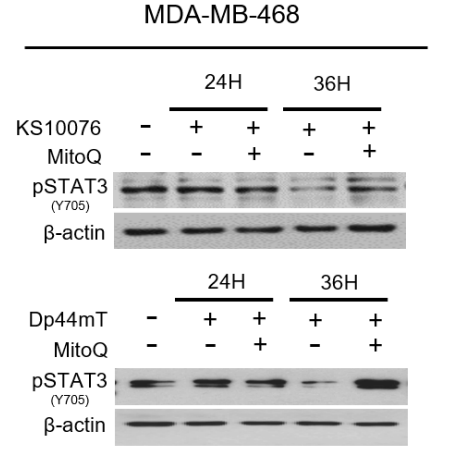

E

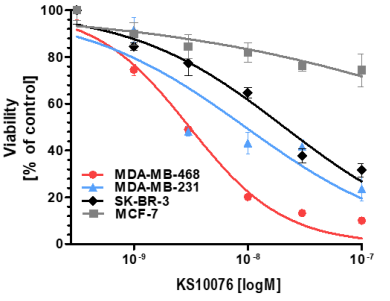

Cell lines	IC_{50} (nM)
MDA-MB-468	3.082
MDA-MB-231	9.518
SK-BR-3	20.95
MCF-7	N/A

F

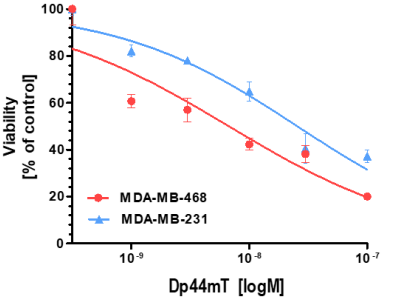

Cell lines	IC_{50} (nM)
MDA-MB-468	6.718
MDA-MB-231	25.56

G

MDA-MB-468

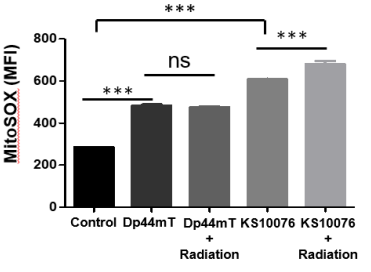

MDA-MB-231

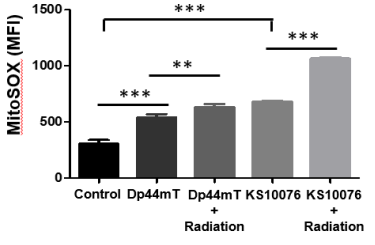

H

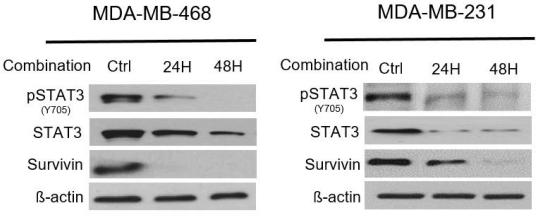

Fig.2 KS10076 suppress pSTAT3 via ROS generation in triple-negative breast cancer cells. (A) Fluorescence of cytosolic iron with calcein green. (B) Cells were treated with KS10076. After 24 h, the level of mitochondrial ROS was determined by measuring the mean fluorescence intensity (MFI) of Mito-SOX. (C) Protein levels of pSTAT3, STAT3, Survivin in MDA-MB-468 cells treated with Dp44mT for 24 h, 48 h. (D) Cell were treated with indicated concentrations of KS10076 in the absence or presence of MitoQ for 24 h, 36 h. (E) Cell viability (CCK-8) in two TNBC cells (MDA-MB-468, MDA-MB-231) and two non-TNBC (SK-BR-3, MCF-7) cells incubated with increasing concentration of KS10076 for 48 h. Results are expressed as the mean of cell viability percentage with respect to the corresponding untreated cell line (100%) ± SEM (n=4). (F) Cell viability (CCK-8) in two TNBC cells (MDA-MB-468, MDA-MB-231) incubated with increasing concentration of Dp44mT for 48 h. (G) Protein levels of pSTAT3, STAT3, Survivin in MDA-MB-468 and MDA-MB-231 cells treated with KS10076 and radiation for 24 h, 48h. (H) Cells were treated with 4 Gy radiation and Dp44mT or KS10076. After 24 h, the level of mitochondrial ROS was determined by measuring the mean fluorescence intensity (MFI) of Mito-SOX. Data were presented as mean ±SD; n=3. P value was determined by one-way ANOVA; ns not significant.

5. KS10076 induces cell death via ER stress in TNBC cells.

To investigate the cell death mechanism by KS10076, KS10076 was treated in MDA-MB-468 and MDA-MB2-231 cells to observe the cell death markers. KS10076 reduced Bcl2, Survivin, XIAP, apoptosis markers, and increased LC3B-II/LC3B-I ratio, autophagy marker (Fig.3A, Fig.S1). Endoplasmic reticulum (ER) stress led to cancer cell death through ATF4-induced autophagy and CHOP-induced[19,20]. In our previous study also reported that KS10076 promoted autophagic cancer cell death via ATF4-eIF2a signaling[32]. Therefore, to investigate whether KS10076 causes ER stress-mediated death in BC cells, we examined the protein expression of ER stress-associated signaling by KS10076 in MDA-MB-468 and MDA-MB-231 cells. The expression of ER stress signaling markers, PERK, peIF2a, ATF4, and CHOP proteins, were up-regulated in both cells at 24 h after KS10076 treatment (Fig.3B). Radiation treatment, on the other hand, did not cause ER stress in MDA-MB-468 cells but did activate the PERK-peIF2a-ATF4 axis in MDA-MB-231 cells (Fig.3B). Despite these differences, the critical indicator of autophagy, the LC3B-II/LC3B-I ratio, was decreased in both cells after radiation treatment. We observed that MDA-MB-231 cells had a lower basal expression of pSTAT3 and generated more ROS than MDA-MB-468 cells when treated with radiation. Thus, we speculated that radiation treatment induced an incomplete ER stress response in MDA-MB-231 cells (PERK, peIF2a, ATF4). However, KS10076 was able to promote a complete ER stress (PERK, peIF2a, ATF4, CHOP) and significantly increase the LC3B-II/LC3B-I ratio in both cell lines (Fig.3B, Fig.S1). Moreover, co-treatment of KS10076 with radiation enhanced the ER stress response and increased the LC3B-II/LC3B-I ratio (Fig.3B, Fig.S2). We demonstrated that KS10076 was capable of increasing TNBC's sensitivity to radiation treatment which ultimately lead to complete ER stress.

ROS promotes ER stress, which in turn induces mitochondrial ROS[21]. To elucidate the mechanistic order of ROS production and ER stress, cells were

incubated with MitoQ prior to KS10076 treatment. The results showed that MitoQ significantly attenuated KS10076-induced activation of PERK, peIF2a, as well as ATF4, and CHOP. The identical results were seen when treated in combination (Fig.3C and Fig.S3). Together, these data indicate that mitochondrial ROS plays a major role as an upstream regulatory molecule in ER stress.

Furthermore, to explore the crosstalk between ER stress and autophagy by KS10076, we detected protein level by silencing the autophagy-related protein ATF4 during ER stress. Knockdown of ATF4 clearly decreased KS10076-induced LC3B-II expression (Fig.3D). These data suggest that KS10076-induced ER stress leads to autophagy through the PERK-eIF2a-ATF4 pathway.

A

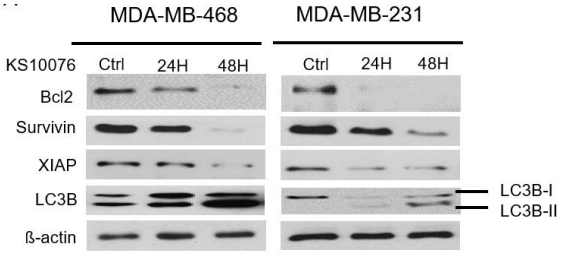

C

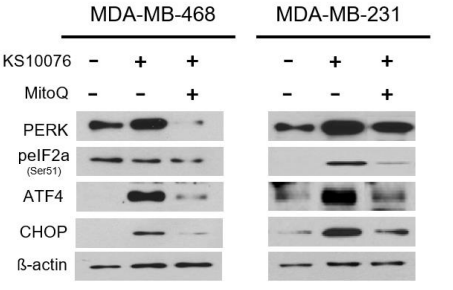

B

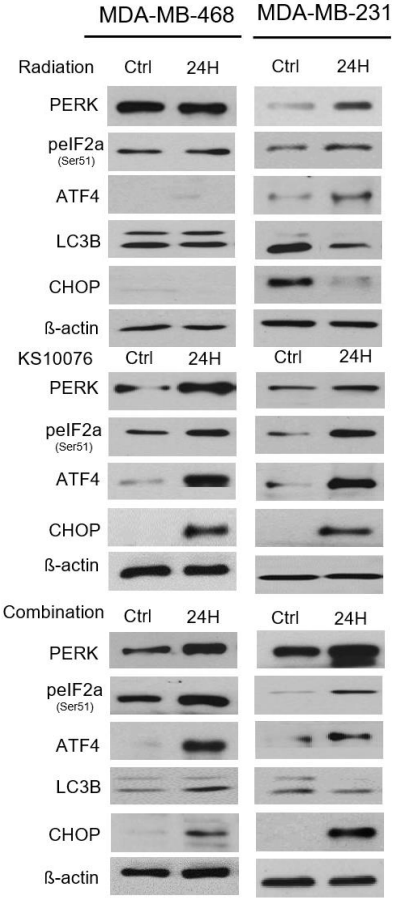

D

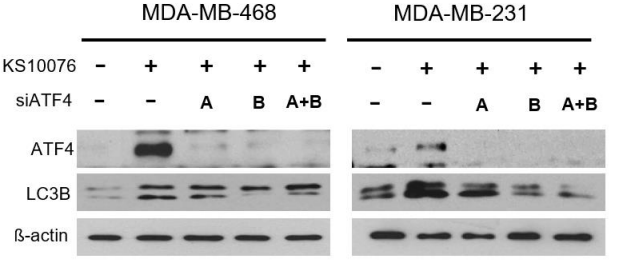

Fig.3 KS10076 induces autophagy and apoptosis via ER stress pathway. (A) Western blot analysis of autophagy and apoptosis markers in MBA-MB-468 and MDA-MB-231 cells. (B) Representative images of Western blot in five groups for selected genes involved in ER stress (PERK, peIF2a, ATF4, CHOP) and autophagy (LC3B). (C) Western blot analysis revealed that MitoQ reversed the expression of the PERK-ER stress proteins. (D) After knockdown of ATF4, MDA-MB-468 and MDA-MB-231 cells were treated with KS10076 to analyze the activation of autophagy pathway against KS10076-induced ER stress.

6. KS10076 and radiation combination greatly increases ROS generation and ER stress.

Metal chelators bind with intracellular iron and copper to induce ROS while radiation-induced ROS is produced by radiolysis of water or cell component molecules (e.g. DNA)[13,21-24]. Therefore, we evaluated ROS level by treatment of KS10076 and radiation. Cells treated with radiation and KS10076 synergistically increased ROS level compared to individually treated cells (Fig.4A).

Next, we speculated that as higher ROS is generated, the more CHOP-induced apoptosis and ATF4-induced autophagy will occur. To test this hypothesis, we first examined apoptotic/anti-apoptotic proteins in TNBC cell lines, MDA-MB-468 and MDA-MB-231. Interestingly, we found that apoptotic protein Cleaved-caspase3 expression was markedly increased in TNBC cells treated with radiation (Fig.4B). However, at the same time, the anti-apoptotic proteins Survivin and Bcl2 were also upregulated. On the other hand, Survivin and Bcl2 were downregulated with KS10076 treatment alone, while Cleaved-caspase3 had no obvious change (Fig.4B). Importantly, combination treatment of KS10076 and radiation showed an appropriate protein expression flow capable of inducing apoptosis (Fig.4B). Consequentially, KS10076 combined with radiation exhibited remarkable induction of apoptosis (Fig.4C). This finding indicates that higher ROS levels may lead to greater ER stress-induced apoptosis (Fig.4A, B, C). Furthermore, knockdown of ATF4 reduced apoptosis cells co-treated with KS10076 and radiation (Fig.4D) thus, we assessed that the ER stress pathway is a critical role in inducing apoptosis in combination conditions.

To further determine ATF4-induced autophagy, we detected LC3B intensity. We observed the highest LC3B intensity in cells treated in combination, which determined greater ROS production in MDA-MB-468 and MDA-MB-231 cells

(Fig.4E, S4). Corresponding with these data, we also found that combination of KS10076 and radiation could induce synergistic growth inhibition (Fig.4F). Hence, the combination of radiation and KS10076 has a synergistic effect that raises ROS production and consequently increases ER stress-induced anti-tumor activity.

A

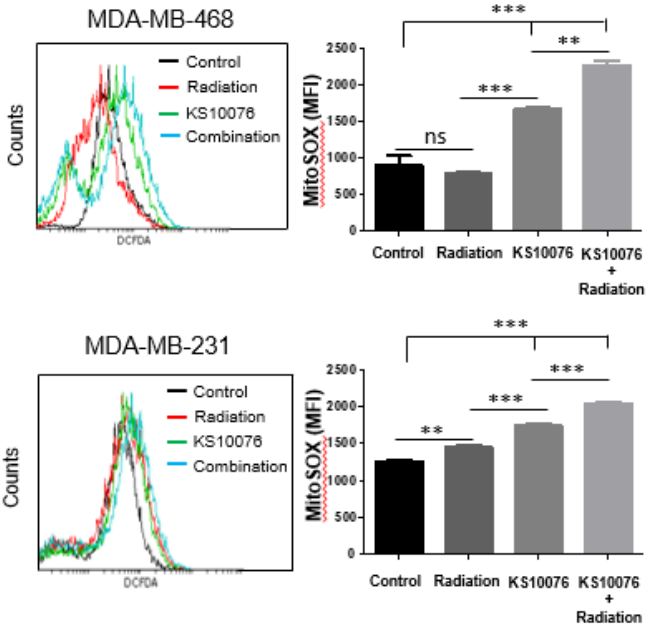

B

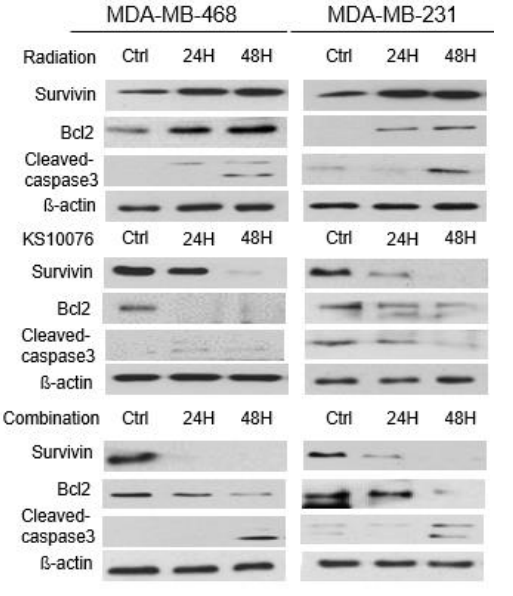

C

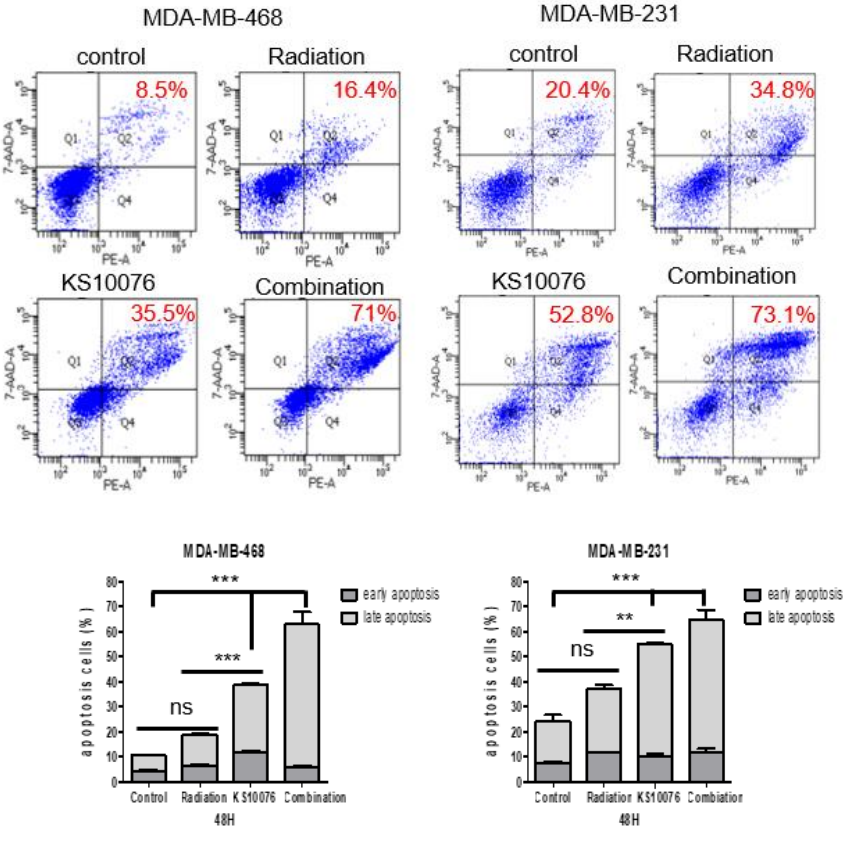

D

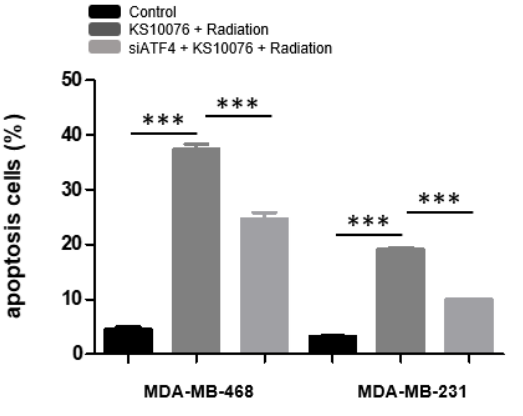

E

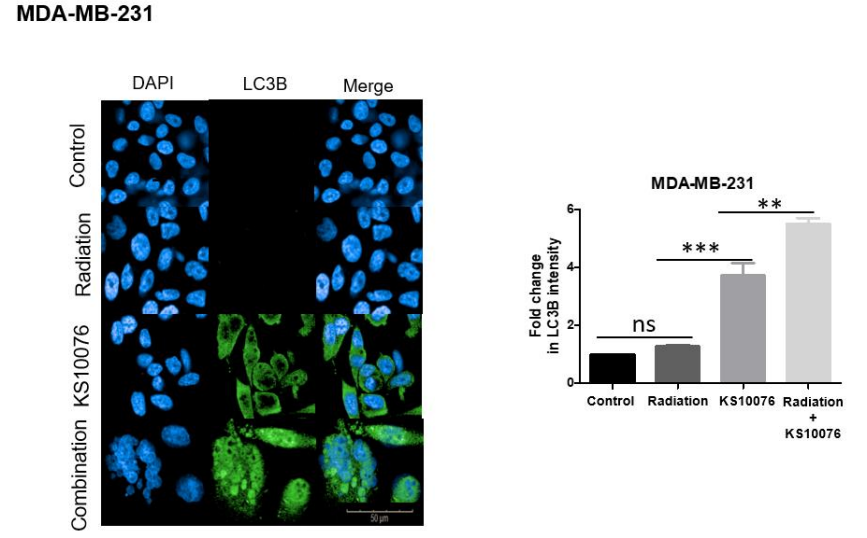

F

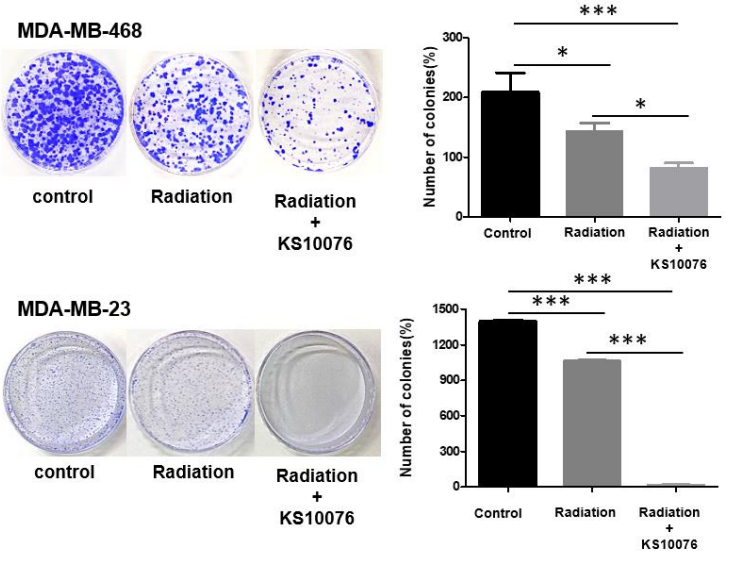

Fig.4 KS10076 and radiation treatment act synergistically effects. (A) Flow cytometry analysis showing cellular ROS levels in TNBC cells. Cells were treated with radiation or KS10076 or radiation + KS10076. (B) Western blot analysis of apoptosis markers in MBA-MB-468 and MDA-MB-231 cells. (C) MDA-MB-468 and MDA-MB-231 cells were treated with radiation or KS10076 or radiation + KS10076 for 48 h, then subjected to flow cytometry analysis of apoptosis. (D) MDA-MB-468 and MDA-MB-231 cells were pretreated with siATF4 24 h. Next, KS10076 and radiation for 48 h, then subjected to flow cytometry analysis of apoptosis. (E) Immunofluorescence results of LC3B distribution in MDA-MB-231 cells treated with KS10076 for 48 h. (E) Clonogenic survival assay in MDA-MB-468 and MDA-MB-231 cells treated with IR alone (4 Gy), KS10076 alone (0.01 μM) of IR + KS10076 (4 Gy and 0.01 μM). Data were presented as mean ±SD; n=3. P value was determined by one-way ANOVA; ns not significant.

7. Overexpression of STAT3 enhances radioresistance against radiation-induced ER stress in non-TNBC cells.

To clarify that the expression of pSTAT3 negatively regulates ER stress, in this study, for the first time, we compared radiation-induced ER stress between TNBC and non-TNBC cells. We found that ROS production is more triggered in non-TNBC cells (SK-BR-3 and MCF-7) which have inherently low pSTAT3 and do not have significant activation of pSTAT3 by radiation, compared to TNBC cells (MDA-MB-468 and MDA-MB-231) (Fig. 1D, G). Consistent with these data, treatment of radiation alone induced-ER stress in SK-BR-3 and MCF-7 cells (Fig.5A, B). To directly investigated whether STAT3 functionally impedes the ER stress pathway, we conducted overexpression of STAT3 in MCF-7 cells. MCF-7 cells overexpressing STAT3 persistently activates the protein expression of pSTAT3 and did not have any ER stress induction (Fig.5B). These data consistently suggested that STAT3 in BC cells affects ROS-induced ER stress through radiotherapy and plays an important role in inducing radioresistance.

A

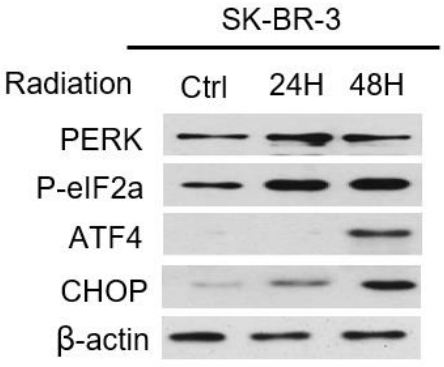

B

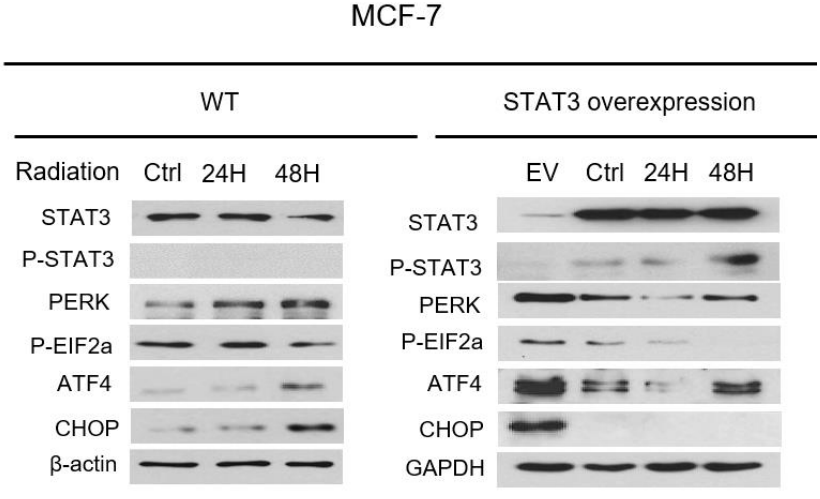

Fig.5 STAT3 decreases ER stress activity. (A) Representative images of Western blot in four groups for selected genes involved in ER stress (PERK, peIF2a, ATF4, CHOP) in SK-BR-3 cells. (B) Western blotting of the indicated proteins in vector control or STAT3-overexpressiong MCF-7 cells with radiation.

8. KS10076 sensitizes xenograft TNBC tumors to radiation.

Finally, we evaluated the therapeutic effect of combination of radiation (6Gy) and KS10076 in vivo. To explore synergistic effect with KS10076 and radiation treatment and to minimize drug toxicity, we used KS10076 at a much lower concentration compared to our previous study. Nude mice were implanted with MDA-MB-231 cells and treated with KS10076 and/or radiation. Over a period of 15 days, co-treatment with KS10076 and radiation significantly inhibited tumor growth and tumor weight, compared to single-agent treatment with no change in body weight (Fig.6A, 6B). In addition, co-treatment markedly reduced tumor volume and tumor weight compared with radiation treatment group (Fig.6A). Furthermore, the low-dose KS10076 group had more inhibition efficacy of the tumor growth than the radiation group (Fig.6A). Collectively these results indicated that co-treatment with KS10076 and radiation significantly reduce tumor growth in vivo via inhibition of STAT3 signaling.

A

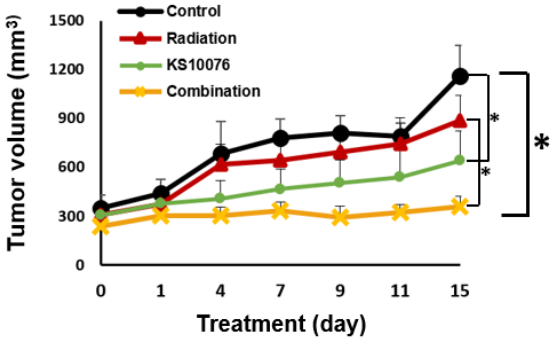

B

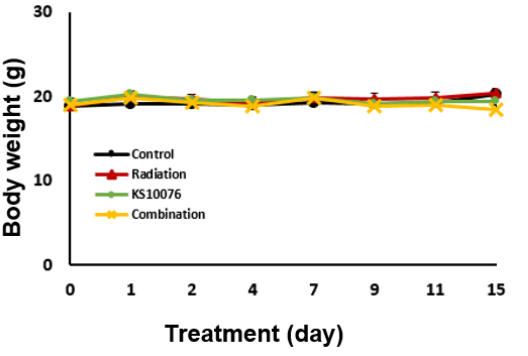

C

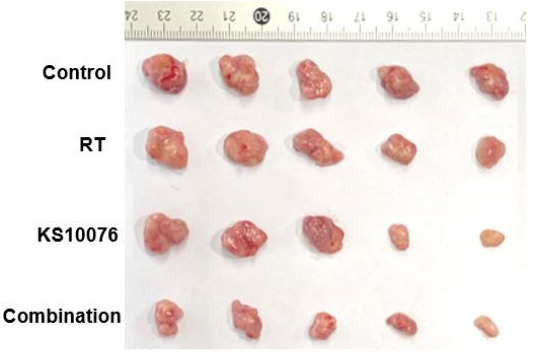

D

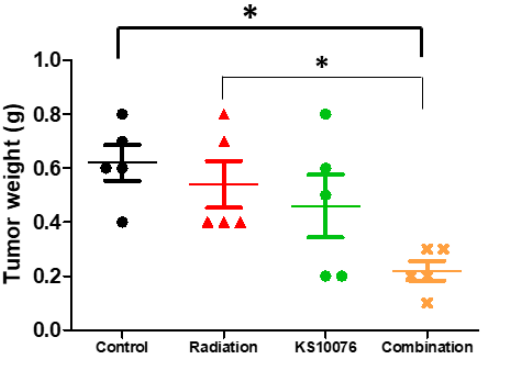

Fig.6 In vivo antitumor effect of combination therapy with KS10076 and ionizing radiation in MDA-MB-231 xenograft tumor models. (A) MDA-MB-231 cells (1.5×10^7 cells/mouse) was subcutaneously inoculated in to the right fat pad of mice. When tumors reached 300 mm^2 in diameter, tumor-bearing mice were irradiated at 6 Gy after treatment with an i.p. injection of KS10076 (12.5 mg/kg) for two cycles every week (arrows indicate each treatment administration). (A, B) Tumor volumes and body weight were calculated every 3 days. (C) Image of xenograft tumor. (D) The dot graph shows dissected tumor weights at the end of experiment. Each dot represents the tumor mass from one mouse ($n = 5$). β-actin was used as an internal control. The mock treatment group was sacrificed on day 15 in the MDA-MB-231 tumor models. P value was determined by t-test; ns not significant. ***P<0.001 vs. control **P<0.01 vs. control *P<0.05 vs. control

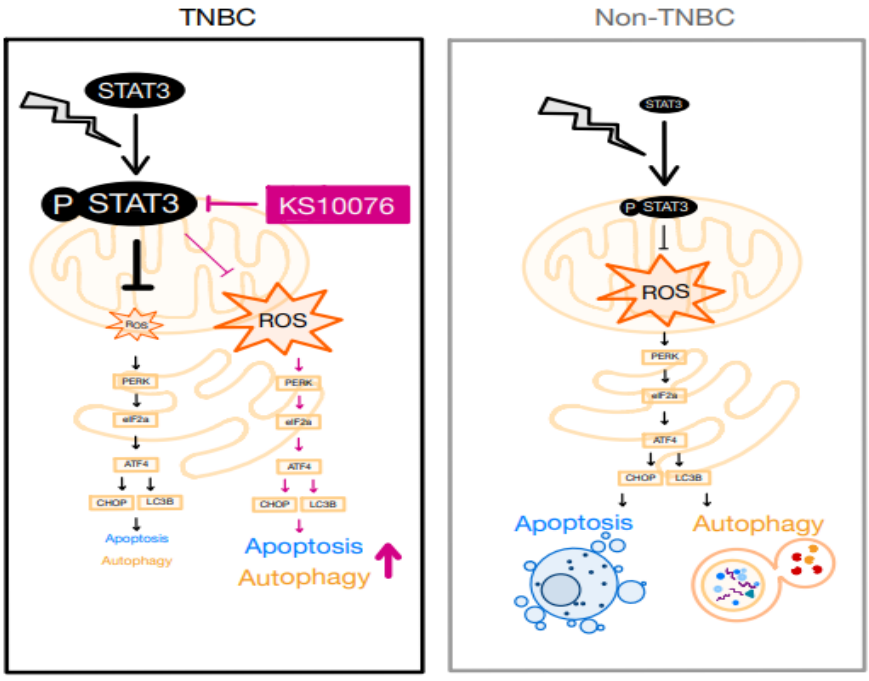

Fig.7 Schematic of crosstalk between pSTAT3 and ROS and activation of ER stress in TNBC or non-TNBC cells.

IV. Discussion

Radiotherapy (RT) is one of the most common and effective therapeutic methods for breast cancer (BC)[5]. But in TNBC, radiotherapy has shown side effects such as local recurrence and lymph node, thus remains a challenging[4,6]. Currently, numerous research has been examined targetable molecules for overcoming radioresistance TNBC via gene expression profiling[24,25]. Several critical studies have been revealed that STAT3 overexpression and constitutively activation associate with TNBC radioresistance[6,7].

Therefore, combination therapy with radiation and STAT3 inhibitor proposed as a new way to overcome radioresistance. However, there are few STAT3 inhibitors available clinically. In this study, we provided evidence that the novel synthesized KS10076 in a previous study could create synergies in combination with radiation. The combination of KS10076 and radiation in vivo significantly suppressed tumor volume without changing body weight, suggesting that it could be used a clinically applicable radio-sensitizer.

Furthermore, we identified the role of STAT3 in radioresistance via ROS-mediated ER stress and also demonstrated that KS10076 overcome radioresistance via ER stress.

The endoplasmic reticulum (ER) is essential for cell homeostasis by regulating protein synthesis, folding, and delivery. It is well known that mitochondrial dysfunction resulting in ROS production could disrupt protein homeostasis and lead to ER stress[21]. In addition, induction of ER stress enhances ATF4-induced autophagy and CHOP-induced apoptosis. Therefore, mitochondrial ROS and ER stress are important factors that determine cell fate mutually.

Cancer cells have a higher basal ROS level than normal cells, as the antioxidant system of cancer cells is hyperactivates[26]. This phenomenon suggests that cancer cells respond more sensitively to external ROS stimuli. Also, previous studies reported that ROS-inducing drugs can lead to cellular

damage and tumor suppression[27,28]. In this regard, anti-tumor effect have been reached through ROS targeted therapy in our study.

So far, numerous studies have revealed that ER stress signaling regulates STAT3 activation[29,30], however, little information has been available regarding the mechanism of how STAT3 expression contributes to ER stress pathway. Therefore, we examined how STAT3 regulates the ER stress, it was revealed by comparing TNBC and non-TNBC cells in which STAT3 is activated differently. STAT3 has been established to protect TNBC cells against oxidative stress and increase antioxidant systems[18]. Therefore, we verified that inhibition of STAT3 facilitated ROS generation and induced ER stress, which promoted apoptosis and autophagy. A key of our approach, which allowed us to provide crosstalk between radiation-induced STAT3 and ER stress, was the focus on ROS. In TNBC cells, STAT3 is significantly activated by RT. In the increase of the cell's tolerance to RT-induced ROS generation. In contrast, non-TNBC cells had no notable activation of STAT3 by radiation and obviously induced ROS production. Therefore, upon RT exposure, only non-TNBC cells induced the ER stress signaling pathway following an increase in ROS production (Fig.7).

Here, we also identified the role of KS10076, overcoming radioresistance by increasing ROS generation and inhibiting pSTAT3. ROS level was shown to be elevated in TNBC cells and directly affected to PERK-ER stress pathway. In conclusion, with the highest ROS level under the combination conditions, the induction of ER stress-induced apoptosis and autophagy was the largest.

Overall, our findings have important implications stating that STAT3 mediates the potential mechanism of radioresistance in TNBC cells. Therapeutic strategies for overcoming STAT3 resistance will have to consider the mechanism of ER stress-mediated resistance in TNBC cells. In this study, we demonstrated the therapeutic potential of targeting STAT3 in radioresistant TNBC by showing that a potent STAT3 inhibitor significantly induces ER stress.

Reference

1. Ensenyat-Mendez M, Llinàs-Arias P, Orozco JI, Íñiguez-Muñoz S, Salomon MP, Sesé B, et al. Current Triple-Negative Breast Cancer Subtypes: Dissecting the Most Aggressive Form of Breast Cancer. Frontiers in Oncology 2021:2311.
2. Pal SK, Childs BH, Pegram M. Triple negative breast cancer: unmet medical needs. Breast cancer research and treatment 2011;125:627-36.
3. Yin L, Duan J-J, Bian X-W, Yu S-c. Triple-negative breast cancer molecular subtyping and treatment progress. Breast Cancer Research 2020;22:1-13.
4. Azoury F, Misra S, Barry A, Helou J. Role of radiation therapy in triple negative breast cancer: current state and future directions—a narrative review. 2021.
5. Group EBCTC. Effect of radiotherapy after breast-conserving surgery on 10-year recurrence and 15-year breast cancer death: meta-analysis of individual patient data for 10 801 women in 17 randomised trials. The Lancet 2011;378:1707-16.
6. Yao Y, Chu Y, Xu B, Hu Q, Song Q. Radiotherapy after surgery has significant survival benefits for patients with triple- negative breast cancer. Cancer medicine 2019;8:554-63.
7. Bravata V, Cammarata FP, Minafra L, Musso R, Pucci G, Spada M, et al. Gene expression profiles induced by high-dose ionizing radiation in MDA-MB-231 triple-negative breast cancer cell line. Cancer Genomics & Proteomics 2019;16:257-66.
8. Qin J-J, Yan L, Zhang J, Zhang W-D. STAT3 as a potential therapeutic target in triple negative breast cancer: a systematic review. Journal of Experimental & Clinical Cancer Research 2019;38:1-16.
9. Wang X, Zhang X, Qiu C, Yang N. STAT3 contributes to radioresistance in cancer. Frontiers in oncology 2020;10:1120.
10. Son A-R, Ahn J, Song J-Y. Niclosamide enhances ROS-mediated cell death through c-Jun activation. Biomedicine & Pharmacotherapy 2014;68:619-24.
11. Lu L, Dong J, Wang L, Xia Q, Zhang D, Kim H, et al. Activation of STAT3 and Bcl-2 and reduction of reactive oxygen species (ROS) promote radioresistance in breast cancer and overcome of radioresistance with niclosamide. Oncogene 2018;37:5292-304.
12. Gritsko T, Williams A, Turkson J, Kaneko S, Bowman T, Huang M, et al. Persistent activation of stat3 signaling induces survivin gene

expression and confers resistance to apoptosis in human breast cancer cells. Clinical cancer research 2006;12:11-9.
13. Azzam EI, Jay-Gerin J-P, Pain D. Ionizing radiation-induced metabolic oxidative stress and prolonged cell injury. Cancer letters 2012;327:48-60.
14. Jia S, Ge S, Fan X, Leong KW, Ruan J. Promoting reactive oxygen species generation: a key strategy in nanosensitizer-mediated radiotherapy. Nanomedicine 2021;16:759-78.
15. Kan C, Zhang J. BRCA1 mutation: a predictive marker for radiation therapy? International Journal of Radiation Oncology* Biology* Physics 2015;93:281-93.
16. Chou F-J, Chen Y, Chen D, Niu Y, Li G, Keng P, et al. Preclinical study using androgen receptor (AR) degradation enhancer to increase radiotherapy efficacy via targeting radiation-increased AR to better suppress prostate cancer progression. EBioMedicine 2019;40:504-16.
17. Cao Y, Wang J, Tian H, Fu G-H. Mitochondrial ROS accumulation inhibiting JAK2/STAT3 pathway is a critical modulator of CYT997-induced autophagy and apoptosis in gastric cancer. Journal of Experimental & Clinical Cancer Research 2020;39:1-15.
18. An H, Heo JS, Kim P, Lian Z, Lee S, Park J, et al. Tetraarsenic hexoxide enhances generation of mitochondrial ROS to promote pyroptosis by inducing the activation of caspase-3/GSDME in triple-negative breast cancer cells. Cell death & disease 2021;12:1-15.
19. Wang M-G, Fan R-F, Li W-H, Zhang D, Yang D-B, Wang Z-Y, et al. Activation of PERK-eIF2α-ATF4-CHOP axis triggered by excessive ER stress contributes to lead-induced nephrotoxicity. Biochimica et Biophysica Acta (BBA)-Molecular Cell Research 2019;1866:713-26.
20. Iurlaro R, Muñoz- Pinedo C. Cell death induced by endoplasmic reticulum stress. The FEBS journal 2016;283:2640-52.
21. Gu S, Chen C, Jiang X, Zhang Z. ROS-mediated endoplasmic reticulum stress and mitochondrial dysfunction underlie apoptosis induced by resveratrol and arsenic trioxide in A549 cells. Chemico-biological interactions 2016;245:100-9.
22. Lui GY, Kovacevic Z, Richardson V, Merlot AM, Kalinowski DS, Richardson DR. Targeting cancer by binding iron: Dissecting cellular signaling pathways. Oncotarget 2015;6:18748.

23. Lui GY, Kovacevic Z, Menezes SV, Kalinowski DS, Merlot AM, Sahni S, et al. Novel thiosemicarbazones regulate the signal transducer and activator of transcription 3 (STAT3) pathway: inhibition of constitutive and interleukin 6–induced activation by iron depletion. Molecular pharmacology 2015;87:543-60.
24. Zhou Z-R, Wang X-Y, Yu X-L, Mei X, Chen X-X, Hu Q-C, et al. Building radiation-resistant model in triple-negative breast cancer to screen radioresistance-related molecular markers. Annals of Translational Medicine 2020;8.
25. Bravata V, Cammarata FP, Minafra L, Musso R, Pucci G, Spada M, et al. Gene expression profiles induced by high-dose ionizing radiation in MDA-MB-231 triple-negative breast cancer cell line. Cancer Genomics & Proteomics 2019;16:257-66.
26. Perillo B, Di Donato M, Pezone A, Di Zazzo E, Giovannelli P, Galasso G, et al. ROS in cancer therapy: The bright side of the moon. Experimental & Molecular Medicine 2020;52:192-203.Role of reactive oxygen species in tumors based on the ‘seed and soil’ theory: A complex interaction (Review).
27. Zhou D, Shao L, Spitz DR. Reactive oxygen species in normal and tumor stem cells. Advances in cancer research: Elsevier; 2014. p.1-67.
28. Zaidieh T, Smith JR, Ball KE, An Q. ROS as a novel indicator to predict anticancer drug efficacy. BMC cancer 2019;19:1-14.
29. Ghoshal S, Fuchs BC, Tanabe KK. STAT3 is a key transcriptional regulator of cancer stem cell marker CD133 in HCC. Hepatobiliary Surg Nutr 2016;5:201-3.
30. Sheshadri N, Poria DK, Sharan S, Hu Y, Yan C, Koparde VN, et al. PERK signaling through C/EBPδ contributes to ER stress-induced expression of immunomodulatory and tumor promoting chemokines

by cancer cells. Cell death & disease 2021;12:1-14.

31. Kim J, Park A, Hwang J, Zhao X, Kwak J, Kim H, et al. KS10076, a chelator for redox-active metal ions, induces ROS-mediated STAT3 degradation in autophagic cell death and eliminates ALDH1+ stem cells. Cell reports 2022;

Supplement

S1

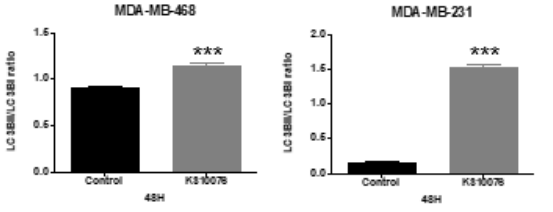

S2

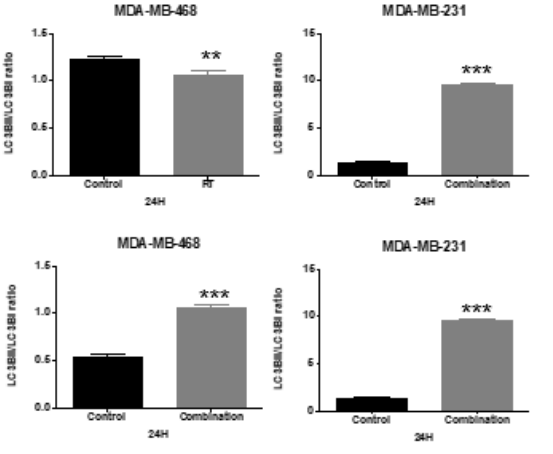

S3

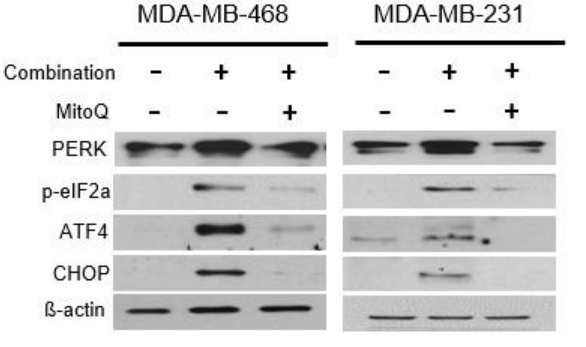

(S1) The ratio of LC3BII to LC3BI in MDA-MB-468 and MDA-MB-231 cells when treated with KS10076 alone. (S2) The ratio of LC3BII to LC3BI in MDA-MB-468 and MDA-MB-231 cells when treated with radiation with or without KS10076 (S3) Western blot analysis revealed that MitoQ reversed the expression of the PERK-ER stress proteins. Results are presented as the mean ± standard error from three independent experiments. P value was determined by t-test; ns not significant. ***P<0.001 vs. control **P<0.01 vs. control *P<0.05 vs. control

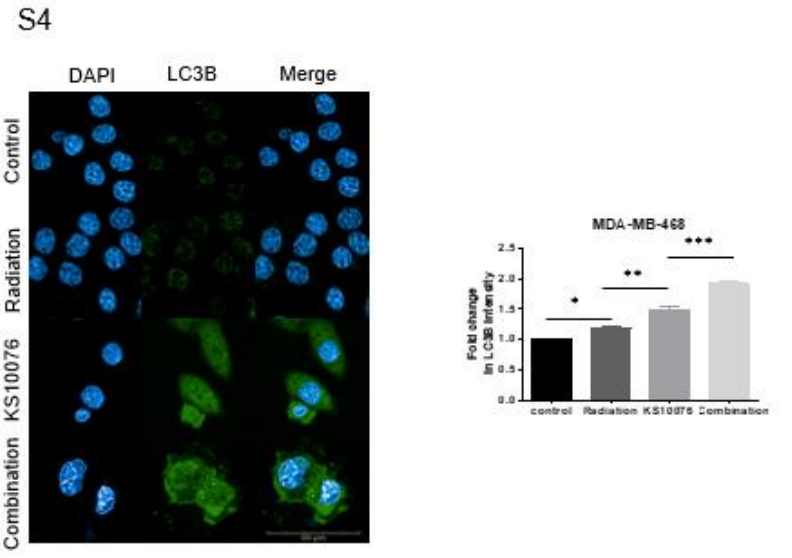

Fig.S4 Immunofluorescence results of LC3B distribution in MDA-MB-468 cells treated with KS10076 for 48 h.

ABSTRACT (IN KOREAN)

금속 킬레이터 KS10076은 삼중 음성 유방암에서 활성 산소 매개 소포체 스트레스 경로를 통해 방사선 감수성을 높인다.

<지도교수 신상준 >

연세대학교 대학원 의학과

유단비

유방암 중 가장 공격적이고 치명적인 삼중 음성 유방암은 방사선치료 에 내성이 있는 것으로 알려져 있으며, STAT3 단백질이 그 내성에 관여한다는 연구결과가 다수 보고되었다. 그러나 STAT3가 방사선 저항을 유도하는 메커니즘은 아직 완전히 이해되지 않았다. 본 연구에서는 처음으로 STAT3 활성화와 소포체 스트레스 사이의 관계를 연관 지어 방사선 내성을 조사하였다. 결과적으로 pSTAT3의 발현이 높은 삼중 음성 유방암 세포에서는 방사선만으로 생성된 활성산소 수준이 낮아, 소포체 스트레스가 유도되지 않는 것으로 나타났다. 반면 pSTAT3 발현이 낮은 비 삼중 음성 유방암 세포는 높은 수준의 활성 산소를 발생시켜, 소포체 스트레스를 유도했다. 더 나아가 우리는 삼중 음성 유방암 세포에 금속 킬레이터, KS10076과 방사선을 병용 처리하면 pSTAT3가 유의하게 감소하고, 활성 산소 생성이 증가하여, 결과적으로 소포체 스트레스 매개 세포자살 및 세포자멸사가 상당한 수준으로 발생하는 것을 관측하였다. 이러한

결과는 KS10076이 활성 산소 매개 소포체 스트레스 증가를 통해 방사선 저항을 극복한다는 것을 암시하였다. 종합하면, 우리의 연구 결과는 방사선 저항과 관련된 새로운 메커니즘을 밝히고, 삼중 음성 유방암 세포에서 방사선 저항을 극복하기 위한 KS10076을 조합 전략을 제공한다.

핵심 되는 말: 삼중음성유방암, STAT3, 방사선, 활성산소, 철 킬레이터, 소포체 스트레스